A Nuclear-Targeted Cameleon Demonstrates Intranuclear Ca^{2+} Spiking in *Medicago truncatula* Root Hairs in Response to Rhizobial Nodulation Factors[1][W][OA]

Björn J. Sieberer, Mireille Chabaud, Antonius C. Timmers, André Monin, Joëlle Fournier, and David G. Barker*

Laboratory of Plant-Microbe Interactions, UMR CNRS-INRA 2594/441, F–31320 Castanet-Tolosan, France (B.J.S., M.C., A.C.T., J.F., D.G.B.); and Laboratory of Systems Analysis and Architecture (LAAS-CNRS), Complexe Scientifique de Rangueil, 31077 Toulouse, France (A.M.)

Lipochitooligosaccharide nodulation factors (NFs) secreted by endosymbiotic nitrogen-fixing rhizobia trigger Ca^{2+} spiking in the cytoplasmic perinuclear region of host legume root hairs. To determine whether NFs also elicit Ca^{2+} responses within the plant cell nucleus we have made use of a nucleoplasmin-tagged cameleon (NupYC2.1). Confocal microscopy using this nuclear-specific calcium reporter has revealed sustained and regular Ca^{2+} spiking within the nuclear compartment of *Medicago truncatula* root hairs treated with *Sinorhizobium meliloti* NFs. Since the activation of Ca^{2+} oscillations is blocked in *M. truncatula* *nfp*, *dmi1*, and *dmi2* mutants, and unaltered in a *dmi3* background, it is likely that intranuclear spiking lies on the established NF-dependent signal transduction pathway, leading to cytoplasmic calcium spiking. A semiautomated mathematical procedure has been developed to identify and analyze nuclear Ca^{2+} spiking profiles, and has revealed high cell-to-cell variability in terms of both periodicity and spike duration. Time-lapse imaging of the cameleon Förster resonance energy transfer-based ratio has allowed us to visualize the nuclear spiking variability in situ and to demonstrate the absence of spiking synchrony between adjacent growing root hairs. Finally, spatio-temporal analysis of the asymmetric nuclear spike suggests that the initial rapid increase in Ca^{2+} concentration occurs principally in the vicinity of the nuclear envelope. The discovery that rhizobial NF perception leads to the activation of cell-autonomous Ca^{2+} oscillations on both sides of the nuclear envelope raises major questions about the respective roles of the cytoplasmic and nuclear compartments in transducing this key endosymbiotic signal.

A key step in the initiation of the root endosymbiotic *Rhizobium*-legume association is the perception by the host plant of specific decorated lipochitooligosaccharides known as nodulation factors (NFs). These bacterial signals activate a number of molecular and cellular responses in root epidermal cells and cortical root tissues that are required for rhizobial infection and/or nodule organogenesis (for review, see Oldroyd and Downie, 2008). NF perception in *Medicago truncatula*

root hairs is necessary for the reorientation of root hair tip growth leading to bacterial entrapment (Esseling et al., 2003) as well as the activation of a signal transduction pathway that leads to the transcription of early nodulin genes such as *ENOD11* (Charron et al., 2004). A central component of this pathway is the triggering of sustained intracellular Ca^{2+} oscillations within the host root hair (for review, see Oldroyd and Downie, 2006). Convincing evidence indicates that this NF-specific calcium spiking response is decoded and transduced by a calcium/calmodulin-dependent kinase (CCaMK), encoded by the *DMI3* gene (for doesn't make infections; Lévy et al., 2004; Gleason et al., 2006). To date three essential *M. truncatula* genes have been shown to function upstream of Ca^{2+} spiking in the NF signal transduction pathway (Wais et al., 2000; Ben Amor et al., 2003). *NFP* (for NF perception; Ben Amor et al., 2003) encodes a LysM receptor-like kinase (LysM-RLK) thought to be directly involved in the perception of NFs. *DMI1* (Catoira et al., 2000; Wais et al., 2000) encodes a putative cation channel (Ané et al., 2004) and *DMI2* a Leu-rich repeat receptor-like kinase of unknown function (Endre et al., 2002). With the exception of *NFP*, these genes are also essential for initial root penetration by arbuscular mycorrhizal fungi, suggesting that the segment of the NF signal

transduction pathway involving Ca^{2+} signaling is conserved between the two endosymbiotic associations (for review, see Oldroyd and Downie, 2004).

Modulations in the levels and localization of intracellular Ca^{2+} in legume root hairs in response to the application of purified NFs have been studied by two approaches. First, dextran-coupled single wavelength calcium-indicator dyes such as Calcium Green or Oregon Green have been microinjected into young growing root hairs (e.g. Wais et al., 2000). Cytoplasmic Ca^{2+} responses were then monitored either directly or via ratio-imaging techniques using a second calcium-insensitive dye such as Texas Red (Shaw and Long, 2003). These experiments revealed that NFs in the nanomolar-to-picomolar concentration range elicit a persistent oscillatory Ca^{2+} response in the host cell cytoplasm, which initiates within 10 min after NF addition to the external medium. High spatial and temporal resolution imaging further showed that the calcium spiking originates in the perinuclear region of the *Medicago* root hair and propagates through the cytoplasm toward the cell tip (Shaw and Long, 2003). More recently, to overcome the many limitations of microinjection, Miwa et al. (2006) have reported the use of a Förster resonance energy transfer (FRET)-based cameleon calcium sensor (YC2.1) to monitor cytoplasmic Ca^{2+} responses in transgenic *M. truncatula* roots. These studies revealed that NFs elicit cell-autonomous perinuclear Ca^{2+} spiking in root hairs and have provided evidence that the number of consecutive calcium spikes may be critical for regulating *ENOD11* gene activation. In the light of these data it was therefore particularly intriguing to discover that DMI3 CCaMK, the presumed Ca^{2+} decoder, locates not to the cytoplasm but to the nuclear compartment of *M. truncatula* root hairs (Smit et al., 2005). This finding rapidly led to the proposal that oscillatory Ca^{2+} signaling must be elicited both within the nucleus as well as around it (for review, see Oldroyd and Downie, 2006, 2008). Although direct experimental evidence for the activation of intranuclear Ca^{2+} spiking in response to NFs is currently lacking, recent research has revealed that animal and plant cell nuclei possess their own calcium stores and associated signaling apparatus and have the potential to generate independent nucleoplasmic Ca^{2+} signatures capable of regulating nuclear-specific cellular processes (for review, see Gomes et al., 2006; Kim et al., 2009; Mazars et al., 2009).

With the specific objective of studying NF-elicited Ca^{2+} signaling responses within the *M. truncatula* nucleus without interference from adjacent perinuclear oscillations, we have made use of a nucleoplasmin-cameleon fusion (NupYC2.1; Watahiki et al., 2004). Confocal FRET-based microscopy using this nuclear-targeted cameleon has shown unequivocally that exogenous NFs trigger persistent Ca^{2+} oscillations within the nucleus of growing root hairs, and that this response is dependent upon functional *NFP*, *DMI1*, and *DMI2* genes. Nuclear Ca^{2+} oscillations are highly variable in terms of frequency and spike duration and the analysis of the spiking profiles for a large population of growing root hairs has been facilitated by the development of a semiautomated mathematical modeling procedure. In addition, we have used time-lapse analysis of Ca^{2+} spiking to directly visualize the cell autonomy and lack of synchrony in adjacent root hairs. Finally, spatio-temporal image analysis has provided evidence that the steep initial increase in the nuclear Ca^{2+} level during spiking originates primarily at the nuclear periphery. These findings raise fundamental questions about the mechanism and role of intracellular Ca^{2+} as a secondary messenger in the NF signal transduction pathway, and in particular the relationship between cytoplasmic and nuclear Ca^{2+} oscillatory responses.

RESULTS

Nucleoplasmin-YC2.1 Specifically Localizes to Nuclei in *M. truncatula* Root Hairs

To target the cameleon Ca^{2+} reporter $YC2.1_{cyt}$ to the nuclear compartment of *M. truncatula* root cells, we made use of a nucleoplasmin-YC2.1 fusion (NupYC2.1) kindly provided by M. Watahiki (Hokkaido University, Sapporo, Japan). This fusion, driven by a pollen-specific promoter, has been used to label vegetative nuclei in *Nicotiana tabacum* pollen tubes (Watahiki et al., 2004). For our experiments, we replaced the pollen-specific promoter by the cauliflower mosaic virus 35S promoter (see "Materials and Methods") and introduced the 35S-NupYC2.1 construct into *M. truncatula* roots via *Agrobacterium rhizogenes*-mediated transformation (Boisson-Dernier et al., 2001). Composite plants with transformed roots expressing NupYC2.1 were then grown on a semisolid support in petri dishes, with the roots covered by a gas-permeable membrane as described in Fournier et al. (2008). Confocal microscopy was used to localize and measure the fluorescence of the cameleon reporter in growing root hairs.

The confocal images presented in Figure 1 show that NupYC2.1 specifically localizes to the nucleus of the root hair, whether in elongating (Fig. 1A) or fully grown hairs (Fig. 1B). Fluorescence is undetectable in the cytoplasm, even within the cytoplasm-dense tip region of elongating root hairs (Fig. 1A). NupYC2.1 fluorescence appears to be homogeneously distributed within the nucleus (with the exception of the nucleolus), and the signal intensity is stable throughout imaging. The high fluorescence level of NupYC2.1 and its excellent signal-to-noise ratio make it possible to perform confocal imaging with reduced laser intensity and fast scanning mode (see "Materials and Methods"). As a result, FRET-based ratio imaging can be performed continuously for up to 40 min with 5 s imaging intervals or for up to 20 min with 1 s imaging intervals without substantial photo bleaching of the nuclear cameleon or any negative effects on root
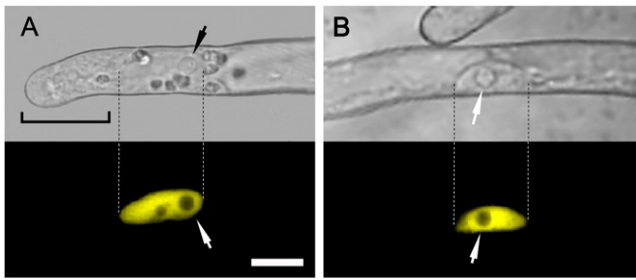
Figure 1. Subcellular localization of the cameleon NupYC2.1 in *M. truncatula* wild-type root hairs. A, Elongating root hair with corresponding confocal fluorescence image showing that the NupYC2.1 labeling is specifically localized in the nucleus. Note that the nucleoli are devoid of fluorescence and that there is no detectable signal in the cytoplasmically dense tip region (bracket). B, Shank of a fully grown root hair in which the NupYC2.1-labeled nucleus is randomly positioned against the cell wall. Dashed lines indicate the nuclear position in corresponding bright-field and fluorescence images. The NupYC2.1 fluorescence is pseudocolored in yellow, and small arrows indicate the position of prominent nucleoli. The magnification is the same for all images. Bar in A is 15 μm.

hair development and growth rate. In conclusion, confocal laser-scanning microscopy using the noninvasive cameleon reporter NupYC2.1 allows direct monitoring of specific changes in nuclear Ca^{2+} levels in *M. truncatula* root hairs at a high temporal and spatial resolution.

NFs Trigger Nuclear Ca^{2+} Spiking in *M. truncatula* Root Hairs

To address the question of whether NFs are able to elicit Ca^{2+} signaling responses within the root hair nucleus, we performed experiments using *A. rhizogenes*-transformed *M. truncatula* plants expressing NupYC2.1, focusing exclusively on growing root hairs with their characteristic cytoarchitecture (Fig. 1A). Following the application of 10^{-9} M *Sinorhizobium meliloti* NFs to composite plant roots, we observed sustained Ca^{2+} spiking within the nucleus for more than 95% of the root hairs examined. As shown in Figure 2, this intranuclear Ca^{2+} response initiated after a variable time delay (average 6 min) and continued over the entire 30 min observation period. Our experiments revealed considerable cell-to-cell variability in the nuclear Ca^{2+} spiking, and this is well illustrated by the examples of low (Fig. 2A) and high (Fig. 2B) frequency oscillatory profiles recorded for two growing root hairs on the same root. The extent of this cell-to-cell variability in terms of the spike periodicity and spike duration is analyzed in more detail in a later section. For approximately 50% of the root hair nuclei examined, the sustained Ca^{2+} spiking was preceded by a short burst of very high frequency spiking (Fig. 2B), which comprised three to six spikes and lasted for less than 2 min. There did not appear to be any correlation between the presence of this initial rapid spiking and

the profile of the subsequent sustained spiking. A broad Ca^{2+} transient was also occasionally observed (approximately 25% of nuclei) preceding the sustained Ca^{2+} oscillations (Fig. 2A).

Cytoplasmic Ca^{2+} spikes generally have asymmetric profiles, resulting from the initial very rapid release of calcium from internal stores such as the endoplasmic reticulum, followed by the much slower pumping of calcium back into the store (Oldroyd and Downie, 2004). The nuclear calcium spike elicited by NFs is also asymmetric, and this is clearly visible in the case of the low-frequency, long-duration spiking profile shown in Figure 2A. To analyze the nuclear spike anatomy in more detail we recorded the onset of nuclear Ca^{2+} spiking using 1 s instead of 5 s imaging intervals. Figure 2, C and D, shows the 1 s resolution spiking profiles for two root hairs that have similar sustained spiking frequencies. In the case of Figure 2C the main spiking is preceded by a short high-frequency spiking sequence. The higher temporal resolution reveals that during spiking, the nuclear Ca^{2+} concentration reaches a maximum level within only a few seconds (irrespective of the spike frequency). In conclusion, rhizobial NFs trigger sustained, regular, and asymmetric Ca^{2+} oscillations within the root hair nucleus.

nfp, *dmi1*, and *dmi2* Mutants Are Defective in NF-Elicited Nuclear Ca^{2+} Spiking

Since cytoplasmic Ca^{2+} spiking lies on the well-characterized NF transduction pathway that ultimately leads to the activation of host genes such as *MtENOD11*, we evaluated nuclear Ca^{2+} responses in mutant lines defective for each of the three *Medicago* genes (*NFP*, *DMI1*, and *DMI2*) that lie upstream of cytoplasmic Ca^{2+} spiking, as well as for the downstream *DMI3* gene encoding the presumed CCaMK calcium decoder. Figure 3 shows that *nfp*, *dmi1*, and *dmi2* mutants are all defective for the NF-elicited nuclear Ca^{2+} responses described above. In contrast, growing root hairs of the *dmi3* mutant responded with sustained nuclear calcium spiking (Fig. 3). Furthermore, as for the wild type, approximately 50% ($n = 18$) of the *dmi3-1* nuclei showed an initial high-frequency spiking sequence. In conclusion, since NF-elicited nuclear Ca^{2+} spiking is dependent upon the identical genes as the cytoplasmic response, it is likely that the same signal transduction pathway is responsible for triggering calcium signaling in both cellular compartments.

Variability and Cell Autonomy of Nuclear Ca^{2+} Spiking in Root Hairs

As illustrated in Figure 2, the nuclear Ca^{2+} spiking profiles elicited in root hairs can vary significantly both in terms of the initial transient responses and the subsequent patterns of sustained spiking. These differences are not a reflection of the developmental stage of the root hair, since we selected only actively grow-
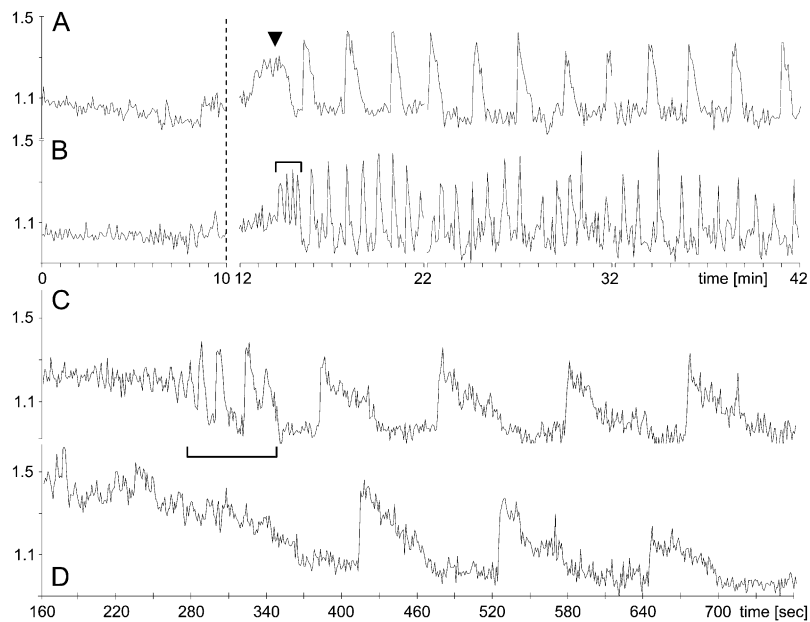
Figure 2. Intranuclear Ca^{2+} spiking in NF-treated root hairs of *M. truncatula*. Root hair nuclei were labeled with NupYC2.1 and imaged with confocal laser-scanning microscopy. Data are presented as YFP-to-CFP ratios (arbitrary units). In A and B, the nuclei of two hairs from the same root were imaged at 5 s intervals for 10 min prior to 10^{-9} M NF treatment (indicated by the dashed line) and then after treatment for 3 × 10 min. A, Example of low-frequency Ca^{2+} spiking with broad spikes. B, Example of high-frequency Ca^{2+} spiking with narrow spikes. The sustained Ca^{2+} spiking is often preceded by a transient high-frequency spiking sequence (bracketed in B) or less frequently by a broad Ca^{2+} transient (arrowhead in A). In C and D, the nuclei of two adjacent hairs were imaged after NF treatment at the higher resolution of 1 s intervals over a 10 min period. C, The sustained Ca^{2+} spiking profile is preceded by a high-frequency Ca^{2+} spiking transient. D, Similar Ca^{2+} spiking profile as in C, but lacking the initial high-frequency transient. Note the very steep increase of the ratio plots at the onset of each individual spike, followed by a slow return to resting levels. For microscopy settings see "Materials and Methods." Time intervals in A and B are in minutes and in C and D the time scale (in seconds) refers to the time following NF treatment.

ing hairs with their characteristic polarized cytoarchitecture (Fig. 1A). To investigate the extent of this spiking variability and also whether the NF concentration can influence the nuclear Ca^{2+} spiking response, we performed parallel experiments on more than 70 root hairs treated with either 10^{-9} or 10^{-11} M NF. The concentration of 10^{-11} M was chosen because this was the lowest NF concentration for which we could still observe clear spiking responses for over 90% of the growing root hairs. To analyze the Ca^{2+} spiking profiles in detail we developed a mathematical algorithm capable of automatically identifying spikes and measuring their duration (see "Materials and Methods" and Supplemental Protocol S1). A histogram representing the distribution of the average calcium spiking periodicities for individual root hairs is presented in Figure 4. Although spiking periodicities range from below 30 s to above 200 s, the majority of root hairs (approximately 90%) display spiking periodicities that lie between 50 and 150 s. The spike duration can also be highly variable, but the majority of spikes last for between 15 and 40 s (data not shown). Lower spiking frequencies generally correlated with longer spike durations as illustrated in Figure 2, A and B. These experiments also revealed that the lag time

between NF addition and the initiation of the sustained spiking varied considerably between 3.5 and 12 min. Although the data presented in Figure 4 initially suggested that there may be differences in the distribution of nuclear spiking frequencies as a function of the NF concentration, statistical analysis was unable to identify significant differences due to the high variability between root hairs and between individual plants. Finally, it should be noted that while the early broad calcium transient was totally absent in nuclei of 10^{-11} M NF-treated root hairs, the short-duration high-frequency response was still observed in over 50% of the root hairs examined.

To visualize the cell-to-cell variability in nuclear calcium spiking in situ we created time-lapse movies of the relative changes in the intranuclear yellow fluorescent protein (YFP)-to-cyan fluorescent protein (CFP) ratios in adjacent growing root hairs throughout several spiking cycles. Supplemental Movie S1 illustrates the Ca^{2+} spiking responses over time for a total of six root hair nuclei following treatment with 10^{-9} M NF. This representation clearly shows the cell-to-cell variability in nuclear spiking between adjacent root hairs and the absence of spiking synchrony. Taken together, these data illustrate the cell-autonomous
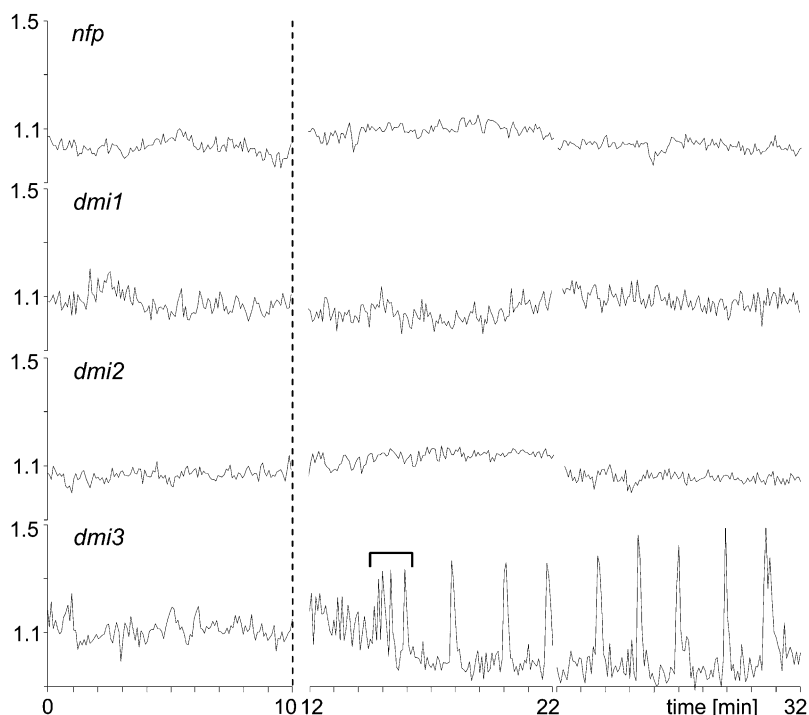
Figure 3. Nuclear Ca^{2+} responses in root hairs of the *M. truncatula* mutants *nfp-2*, *dmi1-1*, *dmi2-2*, and *dmi3-1* following NF treatment. Root hairs were imaged with confocal laser microscopy at 5 s intervals for 2 × 10 min following 10^{-9} M NF treatment. Profiles are YFP-to-CFP ratios (arbitrary units) for nuclear-localized NupYC2.1. The *nfp*, *dmi1*, and *dmi2* mutants are totally defective in nuclear Ca^{2+} responses, whereas the *dmi3* root hair responds with sustained Ca^{2+} spiking. In this particular profile the main spiking is preceded by a high-frequency transient Ca^{2+} spiking sequence (bracketed) as often observed for the wild type. The dashed line indicates the time of NF application, and the time intervals are in minutes.

nature of NF-elicited calcium spiking within the nuclear compartment, as well as the extent of cell-to-cell variability in terms of the time lag prior to induction, the spiking frequency, and the spike duration, even among neighboring root hairs.

Spatio-Temporal Analysis of NF-Elicited Nuclear Ca²⁺ Spiking

Visualizing Ca^{2+} oscillations in the form of a time-lapse movie can also provide valuable information about the spatio-temporal localization of this secondary messenger within the nucleus throughout the different phases of the spike. This is illustrated in Supplemental Movie S2, which shows both the distribution and intensity of the relative changes in the nuclear NupYC2.1 FRET signal for a single NF-treated root hair over a 10 min period with sampling at 5 s intervals. In addition to the expected very rapid buildup in Ca^{2+} concentration within the nucleus, this time-lapse provides a clear indication that the FRET-signal ratio increases preferentially at the periphery of the nuclear compartment during this initial phase of the oscillation.

To improve the temporal resolution we then imaged nuclei at 1 s intervals for up to 15 min and analyzed 40 individual spikes corresponding to the sustained spiking response from six different nuclei. A qualitative frame-by-frame analysis of the relative changes in the YFP-to-CFP ratio in NF-treated nuclei for a single spike is shown in Figure 5 and for eight consecutive spikes in Supplemental Figure S1. These images confirm that the initial very rapid Ca^{2+} increase occurs

primarily in the vicinity of the nuclear envelope (NE). Maximum ratio changes were reached within a few seconds inside the nucleus (e.g. Fig. 5, frames 7–9), although it should be underlined that these steep ratio changes are not uniformly distributed throughout the nucleus (e.g. Fig. 5, frame 7). Following the peak, which only lasts for several seconds, the relatively lengthy return to resting levels appears to initiate within the nuclear core region before reaching the nuclear periphery. In conclusion, spatio-temporal analysis of nuclear spiking provides evidence that the Ca^{2+} increase initiates predominantly at the periphery of the nucleus.

DISCUSSION

Rhizobial NFs Trigger Sustained Nuclear Ca²⁺ Spiking in Root Hairs

Since its initial discovery over a decade ago by Ehrhardt et al. (1996), NF-elicited cytoplasmic Ca^{2+} spiking in legume root hairs has been studied in considerable detail and integrated into a complex and still poorly understood signal transduction pathway leading from NF perception to specific gene expression (for review, see Oldroyd and Downie, 2006). In this article we have addressed the question of whether NFs also activate oscillatory calcium signaling within the nuclear compartment of the host cell by expressing a nucleoplasmin-tagged cameleon (NupYC2.1) calcium sensor in *M. truncatula* roots. The strong expression of NupYC2.1 in *M. truncatula* root hair nuclei and the localization of the cameleon to this
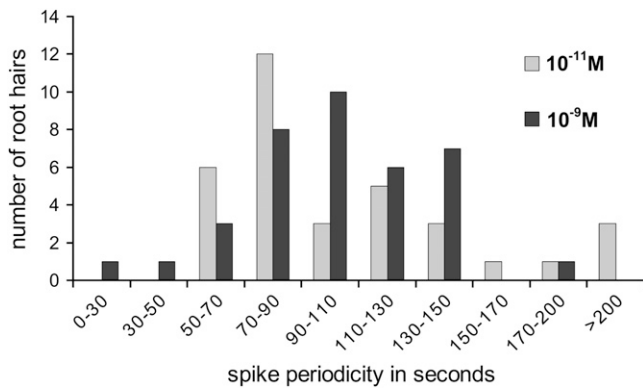
Figure 4. Variability of the spike periodicity for elongating root hairs treated with either 10^{-9} or 10^{-11} M NF. Spike periodicities were averaged over 20 min, starting 10 min after NF treatment. Statistical analysis did not reveal significant differences between the two NF concentrations in relation to the spike frequency.

compact and well-defined intracellular compartment has facilitated the FRET measurements and allowed high temporal resolution studies. Most importantly, the specific targeting of NupYC2.1 to the nucleus has made it possible to monitor NF-elicited changes in nuclear Ca^{2+} levels without interference from perinuclear Ca^{2+} oscillations in the root hair cytoplasm. The absence of detectable NupYC2.1 fluorescence in the cytoplasm means that FRET-related changes in the YFP-to-CFP ratio can only result from intranuclear modulations in Ca^{2+} concentration. Finally, as previously shown for the YC2.1 cytoplasmic cameleon (Miwa et al., 2006), the use of this type of reporter means that Ca^{2+} responses can be observed simultaneously for many root hairs following NF application without perturbing cell development.

Our experiments show that the addition of NFs to growing root hairs triggers sustained and regular Ca^{2+} spiking within the nuclear compartment. Ca^{2+}

spiking profiles are highly variable between individual root hairs, with 90% of hairs displaying spiking periodicities in the range between 50 and 150 s. This is approximately the same frequency range as that described for cytoplasmic perinuclear spiking in *M. truncatula* root hairs (Miwa et al., 2006). Considerable cell-to-cell variability has been observed in relation to the duration of the nuclear Ca^{2+} oscillations (between 15 and 40 s for 90% of root hairs), and the delay that precedes the initiation of the sustained spiking (from 3.5–12 min). For more than 50% of the root hairs examined, the initiation of sustained nuclear Ca^{2+} spiking in response to both 10^{-9} and 10^{-11} M NFs is preceded by a short burst of high-frequency spiking lasting for less than 2 min. Although this has not been referred to previously in the context of cytoplasmic spiking, a similar high-frequency spiking sequence can often be identified in published profiles prior to the initiation of the regular and persistent perinuclear oscillations in legume root hairs (e.g. Wais et al., 2002; Shaw and Long, 2003). The significance of this brief oscillatory sequence is currently unclear, although it is obviously not essential for the initiation of the sustained spiking. The same is true for the early broad transient that is occasionally observed in root hair nuclei after treatment with 10^{-9} M NF, but absent following 10^{-11} M treatment. Finally, time-lapse visualization of NF-elicited Ca^{2+} spiking in nuclei of adjacent growing root hairs clearly shows that these responses are nonsynchronous. The cell-autonomous nature of the calcium signaling response to NFs has also been noted for perinuclear spiking in *M. truncatula* (Miwa et al., 2006).

The absence of nuclear Ca^{2+} spiking in *M. truncatula* lines defective in the *NFP*, *DMI1*, and *DMI2* genes strongly suggests that the well-characterized signal transduction pathway initiated by LysM-RLK-mediated NF perception leading to cytoplasmic Ca^{2+} spiking and the transcriptional activation of specific *ENOD* genes is also responsible for activating nuclear Ca^{2+} spiking. This is consistent with the fact that the mutant line

Figure 5. Spatio-temporal YFP-to-CFP ratio changes during a single Ca^{2+} spike within the nucleus of a NF-treated *M. truncatula* root hair. A, Frame-by-frame imaging sequence (1 s intervals) reveals the distribution and intensity of the YFP-to-CFP ratio throughout a complete nuclear Ca^{2+} spike. Initial steep increases in ratio changes occur primarily at the inner periphery of the nucleus (frames 5–8), before reaching maximum levels (frames 9–11). Intranuclear Ca^{2+} then progressively drops to the original resting levels (frames 14–21). B, Graph showing the average YFP-to-CFP ratios of the Ca^{2+} spike shown in A, corresponding to the region of interest drawn over the nucleus (dotted line in inset) that is positioned close to the tip of the growing root hair. Timing in A and B is in seconds. Magnification is the same for all images. Bar in B = 15 μm.
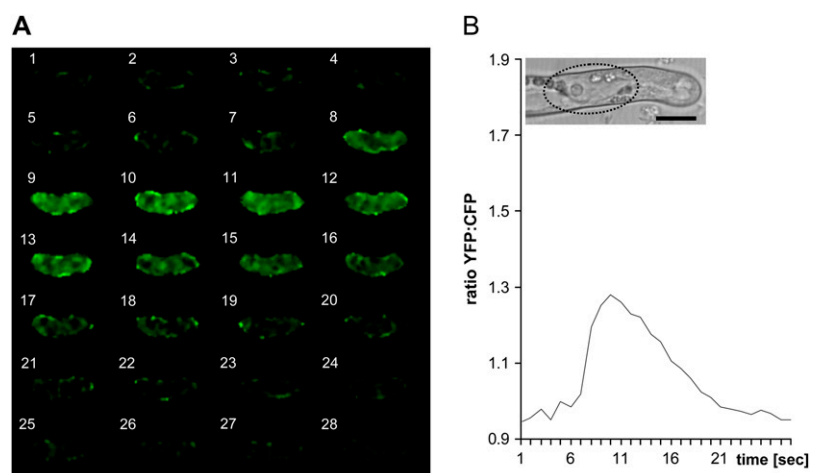
defective in the CCaMK-encoding gene *DMI3* still exhibits NF-elicited nuclear Ca²⁺ spiking. In conclusion, our data indicate that perinuclear and intranuclear Ca²⁺ spiking in *Medicago* root hairs share a number of important features including a common signal transduction pathway, cell-autonomous responses, similar calcium oscillation patterns, and highly variable Ca²⁺ spiking profiles.

What Is the Origin of NF-Dependent Nuclear Ca²⁺ Spiking?

The nucleus is a functionally distinct compartment of the eukaryotic cell that is separated from the cytosol by the NE. This envelope contains nuclear pores that regulate the transport of ions and molecules between the two compartments. In animal cell studies it is now well documented that Ca²⁺ signals can be generated independently in both the cytoplasm and nucleus, and there is good evidence that nuclear Ca²⁺ plays a key role in a wide variety of cellular functions (for review, see Gomes et al., 2006). Although research in this field is less advanced in plants, it is equally clear that cytosolic and nuclear calcium fluxes can be regulated independently and that Ca²⁺ does not diffuse passively across the NE (for review, see Mazars et al., 2009). Part of the evidence favoring this conclusion has come from the observation that external stimuli such as certain proteinaceous elicitors trigger different Ca²⁺ responses in the two compartments of the plant cell (Lecourieux et al., 2005). Equally, periodic fluctuations in cytosolic calcium that are associated with pollen tube tip growth have not been observed in the nuclear compartment (Watahiki et al., 2004). As a result, the discovery that exogenous NFs activate similar Ca²⁺ spiking responses in both the root hair cytoplasm and nucleus is an important finding, and suggests that these sustained regular oscillations are most probably coordinated across the NE.

The spatio-temporal imaging of the NupYC2.1 FRET signal throughout several spiking cycles (Fig. 5; Supplemental Fig. S1) suggests that the rapid increase in nuclear Ca²⁺ levels initiates predominantly at the nuclear periphery. This is consistent with the well-established mechanism in animal cells involving Ca²⁺ release into the nucleus from the lumen of the NE via the transient opening of Ca²⁺ channels located on the inner face of the envelope (Gomes et al., 2006). The spatio-temporal imaging also shows that YFP-to-CFP ratio changes during a nuclear Ca²⁺ spike are not homogeneously distributed throughout the nucleus. Although this could be due in part to the unlabeled nucleolus (Fig. 1), it is also possible that part of the Ca²⁺ release may occur via nuclear grooves and invaginations (Collings et al., 2000) or from intranuclear stores analogous to the nucleoplasmic reticulum of animal cells (Lee et al., 2006). Because Ca²⁺ release inside the nucleus is an extremely rapid process with maxima being reached within seconds, significantly higher resolution imaging will now be needed to perform more detailed spatio-temporal analysis of NF-elicited intranuclear Ca²⁺ spiking.

Integrating Nuclear Ca²⁺ Spiking into the NF Signal Transduction Pathway

Genetic approaches have identified several key NF signal transduction components upstream of Ca²⁺ spiking that are associated with either the NE or the nucleoplasm. *DMI1* encodes a putative cation channel that localizes to the nuclear periphery (Riely et al., 2007). Although DMI1 does not appear to be a Ca²⁺ channel, experiments performed in yeast (*Saccharomyces cerevisiae*) suggest that DMI1 may be involved in regulating Ca²⁺ release (Peiter et al., 2007). It has been proposed that this trans-membrane protein is a K⁺ channel located in the inner membrane of the NE capable of opening voltage-gated Ca²⁺ channels, and that DMI1 might be the target of a secondary messenger generated following NF perception (Oldroyd and Downie, 2008). In *Lotus japonicus*, similar conclusions have been reached for the DMI1 orthologs CASTOR and POLLUX (Charpentier et al., 2008). In addition, mutations in both the *NUP133* and *NUP85* genes of *L. japonicus* are defective in NF-elicited Ca²⁺ spiking (Kanamori et al., 2006; Saito et al., 2007). These two genes are predicted to encode nucleoporins belonging to the central basket structure of the nuclear pore complex, and LjNUP133 has been localized to punctuate structures at the nuclear rim in *Lotus* root hairs (Kanamori et al., 2006). Although the essential role of these two nucleoporins in activating Ca²⁺ spiking remains unclear, it is possible that the nuclear pore complex is required for transporting ions or molecules such as secondary messengers into or out of the nuclear compartment. Alternatively it has been proposed that NUP133/85 may function together to localize inner nuclear membrane proteins such as ion channels (Oldroyd and Downie, 2008). The same authors have suggested that a cytoplasmically generated secondary messenger such as inositol 1,4,5-trisphosphate might be the key molecule transported into the nucleus via nuclear pores that then targets the DMI1 channel and thus triggers Ca²⁺ influx. However, it should also be borne in mind that the animal cell nucleus possesses its own membrane receptors and signal transduction apparatus that includes the generation of secondary messengers such as inositol 1,4,5-trisphosphate and the opening of ligand-operated receptor Ca²⁺ channels located on the inner face of the NE (for review, see Gomes et al., 2006). If this is also the case for plant nuclei, then it is possible that specific receptors located on the outer membrane of the NE may be involved in perceiving and transducing cytoplasmic signals generated following initial NF perception at the plasma membrane.

Once persistent intracellular Ca²⁺ spiking has been initiated, this signal needs to be recognized and transduced into specific cellular responses. There is

good evidence that the key Ca^{2+}-decoding protein during NF signal transduction is the DMI3 CCaMK. This protein can bind calcium both directly and in a complex with calmodulin, and it is thought that this dual binding confers the capacity to recognize an oscillatory Ca^{2+} signal (Oldroyd and Downie, 2004). Most significantly, the removal of the autoinhibitory domain of DMI3 leads to NF-independent constitutive *ENOD* gene expression (Gleason et al., 2006). The transcriptional regulators NSP1 (Smit et al., 2005), NSP2 (Kaló et al., 2005), and ERN1 (Andriankaja et al., 2007; Middleton et al., 2007), as well as the interacting protein IPD3/Cyclops (Messinese et al., 2007; Yano et al., 2008), which are all essential for NF-dependent gene expression, are known to function downstream of DMI3. The fact that all of these proteins including DMI3 localize to the nuclear compartment (NSP2 relocates to the nucleoplasm following NF perception) suggests that the decoding and transduction of the oscillatory Ca^{2+} signal leading to *ENOD* gene expression occurs primarily within the nucleus.

In addition to understanding precisely how nuclear spiking is initiated and maintained, a number of other important questions remain to be addressed. What is the role of NF-elicited cytoplasmic Ca^{2+} spiking and what is the relationship between cytoplasmic and nuclear spiking? As discussed earlier, it is likely that there is extensive interplay between nuclear and cytoplasmic compartments in coordinating cellular responses to extracellular signals and developmental cues. The fact that both *dmi1* and *nup133/85* mutants are defective in Ca^{2+} spiking suggests that cytoplasmic-nuclear trafficking and/or signal transduction across the NE is a prerequisite for the activation and maintenance of Ca^{2+} signaling, whether in the nuclear or cytoplasmic compartments. Evidence from animal cell studies suggests that the nuclear Ca^{2+} response may initially precede its cytoplasmic counterpart, although differences in timing are generally only of the order of several seconds (Echevarria et al., 2003; Leite et al., 2003). Future challenges will therefore include the development of cameleon variants with different FRET pairs targeted to both the nucleus and the cytoplasm to study NF-dependent activation and potential synchronization of Ca^{2+} spiking in these two subcellular compartments.

MATERIALS AND METHODS

Construction of the Nuclear-Targeted YC2.1 Cameleon

To generate the binary plasmid p35S:NupYC2.1-Kan containing the nucleoplasmin-cameleon YC2.1 fusion (NupYC2.1) under the control of the cauliflower mosaic virus 35S promoter and expressing the kanamycin resistance gene, the 2 kb *Xho*I-*Xba*I fragment containing the cameleon YC2.1 sequence was excised from p35S-YC2.1-Kan (Allen et al., 1999; kindly provided by J. Schroeder, University of California, San Diego, CA) and replaced by the 2.7 kb *Xho*I-*Xba*I fragment containing the NupYC2.1 fusion from pART9-NupYC2.1 (Watahiki et al., 2004; kindly provided by M. Watahiki, Hokkaido University, Sapporo, Japan).

Plant Material and *Agrobacterium rhizogenes*-Mediated Root Transformation

In this study, we have used the wild-type *Medicago truncatula* genotype Jemalong A17 and the *M. truncatula* mutants *nfp-2* (Arrighi et al., 2006), *dmi1-1*, *dmi2-2*, and *dmi3-1* (Catoira et al., 2000; Wais et al., 2000).

Agrobacterium rhizogenes transformation was performed according to Boisson-Dernier et al. (2001). Twenty-one days after inoculation, composite plants with a high fluorescence level in root cell nuclei suitable for Ca^{2+} imaging were selected for microscopy studies. The expression of 35S:NupYC2.1 had no detrimental effects on either root growth or root hair development and transformed composite plants were cultivated for periods exceeding 1 month without any loss of fluorescence. All plants were grown in a culture room with a light intensity of 70 $\mu E\ s^{-1}\ m^{-2}$ at 20°C and with a 12-h photoperiod for the first week of transformation, followed by growth at 25°C with a 16-h photoperiod.

Imaging Intranuclear Ca^{2+} Responses to Rhizobial NFs

For in vivo microscopy studies, we exploited the experimental setup previously used for monitoring root hair infection by rhizobacteria of *A. rhizogenes*-transformed *M. truncatula* composite plants (Fournier et al., 2008). Selected composite plants were transferred 4 to 5 d prior to microscopic observation to square petri dishes containing modified Fåhraeus medium (without nitrogen and with the $MgSO_4$ concentration increased to 3 mM) containing 0.5% Phytagel (Sigma). Note that it was not necessary to include the ethylene biosynthesis inhibitor 2-aminoethoxyvinylglycine in the growth medium for these experiments. Roots were covered with a sterile, gas-permeable, and transparent plastic film (BioFolie 25; Sartorius AG, Vivascience) that has the same optical refractive index as water. This allows the use of water-immersion objectives (see below), and limits water evaporation during observation. Roots growing in the thin water layer between the agar surface and the plastic film display very low levels of endogenous fluorescence compared to roots growing in air (Genre et al., 2005). Plants were grown in the culture room with the plates slightly tilted to favor root growth against the plastic film and with the roots protected from light.

NF treatment was performed by adding 2 mL of aqueous NF solutions (10^{-9} or 10^{-11} M) freshly diluted from a concentrated 10^{-3} M ethanol stock (kindly provided by F. Maillet, LIPM, Castanet-Tolosan, France) to the roots between the plastic film and the semisolid medium. Confocal imaging was performed 10 min before NF treatment to assess the background fluorescence levels, and then initiated 2 to 2.5 min following treatment for a total period of up to 30 min. FRET-based ratio imaging for detecting relative changes of Ca^{2+} levels corresponding to changes in CFP and YFP fluorescence intensities (Miyawaki et al., 1997, 1999) in root hair nuclei was performed with a Leica TCS SP2 AOBS confocal laser-scanning microscope (Leica Microsystems GmbH) equipped with a long-distance HCX Apo L NA 0.80 water-immersion objective 40× (Leica).

The NupYC2.1 Ca^{2+} sensor was excited with the argon laser (80% power setting) at 458 nm. Emissions were collected simultaneously in the 470–500 nm range for CFP and the 530–570 nm range for YFP. To obtain still images with high optical xyz resolution, the pinhole was set to 64 μm, the scanning resolution to 512 × 512 pixels, the scanning speed to 400 Hz, and the line average to 2. Images showing the nuclear localization of NupYC2.1 have been pseudocolored in yellow (Fig. 1; Supplemental Fig. S1). For the time series, the pinhole of the microscope was set to 253 μm (corresponding to an optical slice thickness of approximately 6 μm) and images were collected every 1 or 5 s. For the 1 s imaging intervals the scanning resolution was set to 64 × 64 (Fig. 2, C and D; Supplemental Fig. S1) or 128 × 128 pixels (Fig. 5A), and the scanning speed to 800 Hz with each individual image scan lasting 0.261 or 0.34 s, respectively. For the 5 s imaging intervals the scanning resolution was set to either 128 × 128 (Supplemental Movie S2) or 256 × 256 pixels (Supplemental Movie S1), and the scanning speed to 400 Hz with each individual image scan lasting 0.675 or 0.995 s, respectively. Bright-field images were acquired simultaneously using the transmission detector of the microscope. Images were acquired using Leica confocal software and processed using the Leica CS, and ImageJ (http://rsb.info.nih.gov/ij) software. Final cropping, resizing, and mounting of the images were performed with ImageJ or Adobe Photoshop CS2 (Adobe Systems).

Ratio values for visualizing relative changes of the nuclear YFP-to-CFP signal intensities of NupYC2.1 in mounted image series or time-lapse movies were obtained after applying a median filter of 2 pixels radius to CFP and YFP image series, background subtraction, and signal clipping using the Ratio-

plus plug in for ImageJ. The resulting image series of relative ratio changes were adjusted for contrast and brightness, and pseudocolored in green by using ImageJ.

Mathematical-Statistical Tools for Analyzing Intranuclear Ca^{2+} Responses

The NupYC2.1 YFP-to-CFP ratios for line graphs were calculated and plotted over time using Microsoft Office Excel 2003 SP3 (Microsoft Corporation) after importing data from manually drawn regions of interest in the recorded images files using Leica confocal software. We have developed an in-house script for MATLAB R2007b (The MathWorks Inc.) capable of identifying and characterizing the nuclear Ca^{2+} spiking responses elicited by NFs, and allowing the measurement of key parameters such as spike frequency and duration. After testing several mathematical time-dependent functions, we discovered that the asymmetric Ca^{2+} peak could be successfully modeled by a third-order dynamic system defined by $f(t) = t^2 \exp(-t/T)$, where T stands for a time constant. The pattern is then defined by $a + bf((t - \tau)/\sigma)$, where a is the bias (local mean value of the pattern), b is the amplitude of ratio changes depending on the peak signal power, τ is the time delay between ratio changes, and σ is a scale factor. To discriminate between genuine spiking, non-FRET-related spikes, and background noise, we used a pattern recognition algorithm that computes the likelihood for all the parameters (values of a, b, σ, and τ). For a detailed description of this algorithm see Supplemental Protocol S1. Note that, since the additive noise is assumed to be white and Gaussian, this is equivalent to minimizing the quadratic error between the peak signal and the pattern.

The quantitative data extracted from this mathematical analysis in relation to the timing of the various responses, the Ca^{2+} spiking periodicity and the spike duration were collected for a total of 70 root hairs (four plants treated with 10^{-11} M NF and five plants treated with 10^{-9} M NF; between four and 11 root hairs analyzed per plant). Data were subsequently submitted to a statistical analysis using Statgraphics Centurion XV.II professional software (Statpoint technologies Inc.). Normality of residues was verified by the Kolmogorov-Smirnov test (P value > 0.05). The effect of the NF concentration on the periodicity and duration of the spikes was tested by nested factor ANOVA (plant factor nested in the NF concentration).

Supplemental Data

The following materials are available in the online version of this article.

Supplemental Figure S1. High spatio-temporal resolution of oscillating intranuclear Ca^{2+} levels during NF-elicited spiking in a single *M. truncatula* root hair.

Supplemental Movie S1. Visualizing the nuclear Ca^{2+} spiking variability and cell autonomy in adjacent growing root hairs.

Supplemental Movie S2. Spatio-temporal distribution of NF-elicited intranuclear Ca^{2+} spiking in a single *M. truncatula* root hair expressing NupYC2.1.

Supplemental Protocol S1. Pattern recognition algorithm for identifying and measuring Ca^{2+} spikes in YFP-to-CFP ratio line-graph readouts for intracellular cameleon sensors.

LITERATURE CITED

Allen GJ, Kwak JM, Chu SP, Llopis J, Tsien RY, Harper JF, Schroeder JI (1999) Cameleon calcium indicator reports cytoplasmic calcium dynamics in Arabidopsis guard cells. Plant J **19:** 735–747

Andriankaja A, Boisson-Dernier A, Frances L, Sauviac L, Jauneau A, Barker DG, de Carvalho-Niebel F (2007) AP2-ERF transcription factors mediate Nod Factor-dependent MtENOD11 activation in root hairs via a novel cis-regulatory motif. Plant Cell **19:** 2866–2885

Ané JM, Kiss GB, Riely BK, Penmetsa RV, Oldroyd GE, Ayax C, Lévy J, Debellé F, Baek JM, Kalo P, et al (2004) *Medicago truncatula* DMI1 required for bacterial and fungal symbioses in legumes. Science **303:** 1364–1367

Arrighi JF, Barre A, Amor BB, Bersoult A, Soriano LD, Mirabella R, de Carvalho-Niebel F, Journet EP, Ghérardi M, Huguet T, et al (2006) The *Medicago truncatula* lysine motif-receptor-like kinase gene family includes NFP and new nodule-expressed genes. Plant Physiol **142:** 265–279

Ben Amor B, Shaw SL, Oldroyd GED, Maillet F, Varma PR, Cook D, Long SR, Denarie J, Gough C (2003) The NFP locus of *Medicago truncatula* controls an early step of Nod factor signal transduction upstream of a rapid calcium flux and root hair deformation. Plant J **34:** 495–506

Boisson-Dernier A, Chabaud M, Garcia F, Bécard G, Rosenberg C, Barker DG (2001) *Agrobacterium rhizogenes*-transformed roots of *Medicago truncatula* for the study of nitrogen-fixing and endomycorrhizal symbiotic associations. Mol Plant Microbe Interact **14:** 695–700

Catoira R, Galera C, de Billy F, Penmetsa RV, Journet EP, Maillet F, Rosenberg C, Cook D, Gough C, Dénarié J (2000) Four genes of *Medicago truncatula* controlling components of a Nod factor transduction pathway. Plant Cell **12:** 1647–1666

Charpentier M, Bredemeier R, Wanner G, Takeda N, Schleiff E, Parniske M (2008) *Lotus japonicus* CASTOR and POLLUX are ion channels essential for perinuclear calcium spiking in legume root endosymbioses. Plant Cell **20:** 3467–3479

Charron D, Pingret JL, Chabaud M, Journet EP, Barker DG (2004) Pharmacological evidence that multiple phospholipid signaling pathways link Rhizobium Nodulation factor perception in *Medicago truncatula* root hairs to intracellular responses including Ca^{2+} spiking and specific ENOD gene expression. Plant Physiol **136:** 3582–3593

Collings DA, Carter CN, Carter CN, Rink JC, Scott AC, Wyatt SE, Allen NS (2000) Plant nuclei can contain extensive grooves and invaginations. Plant Cell **12:** 2425–2440

Echevarria W, Leite MF, Guerra MT, Zipfel WR, Nathanson MH (2003) Regulation of calcium signals in the nucleus by a nucleoplasmic reticulum. Nat Cell Biol **5:** 440–446

Ehrhardt DW, Wais R, Long SR (1996) Calcium spiking in plant root hairs responding to Rhizobium nodulation signals. Cell **85:** 673–681

Endre G, Kereszt A, Kevei Z, Mihacea S, Kaló P, Kiss GB (2002) A receptor kinase gene regulating symbiotic nodule development. Nature **417:** 962–966

Esseling JJ, Lhuissier FG, Emons AM (2003) Nod factor-induced root hair curling: continuous polar growth towards the point of Nod factor application. Plant Physiol **132:** 1982–1988

Fournier J, Timmers ACJ, Sieberer BJ, Jauneau A, Chabaud M, Barker DG (2008) Mechanism of infection thread elongation in root hairs of *Medicago truncatula* and dynamic interplay with associated rhizobial colonization. Plant Physiol **148:** 1985–1995

Genre A, Chabaud M, Timmers T, Bonfante P, Barker DG (2005) Arbuscular mycorrhizal fungi elicit a novel intracellular apparatus in *Medicago truncatula* root epidermal cells before infection. Plant Cell **17:** 3489–3499

Gleason C, Chaudhuri S, Yang T, Muñoz A, Poovaiah BW, Oldroyd GE (2006) Nodulation independent of rhizobia induced by a calcium-activated kinase lacking autoinhibition. Nature **441:** 1149–1152

Gomes DA, Leite MF, Bennett AM, Nathanson MH (2006) Calcium signaling in the nucleus. Can J Physiol Pharmacol **84:** 325–332

Kaló P, Gleason C, Edwards A, Marsh J, Mitra RM, Hirsch S, Jakab J, Sims S, Long SR, Rogers J, et al (2005) Nodulation signaling in legumes requires NSP2, a member of the GRAS family of transcriptional regulators. Science **308**: 1786–1789

Kanamori N, Madsen LH, Radutoiu S, Frantescu M, Quistgaard EMH, Miwa H, Downie JA, James EK, Felle HH, Haaning LL, et al (2006) A nucleoporin is required for induction of Ca^{2+} spiking in legume nodule development and essential for rhizobial and fungal symbiosis. Proc Natl Acad Sci USA **103**: 359–364

Kim MC, Chung WS, Yun DJ, Cho MJ (2009) Calcium and calmodulin-mediated regulation of gene expression in plants. Mol Plant **2**: 13–21

Lecourieux D, Lamotte O, Bourque S, Wendehenne D, Mazars C, Ranjeva R, Pugin A (2005) Proteinaceous and oligosaccharidic elicitors induce different calcium signatures in the nucleus of tobacco cells. Cell Calcium **38**: 527–538

Lee RKY, Lui PPY, Ngan EKS, Lui JCK, Suen YK, Chan F, Kong SK (2006) The nuclear tubular invaginations are dynamic structures inside the nucleus of HeLa cells. Can J Physiol Pharmacol **84**: 477–486

Leite MF, Thrower EC, Echevarria W, Koulen P, Hirata K, Bennett AM, Ehrlich BE, Nathanson MH (2003) Nuclear and cytosolic calcium are regulated independently. Proc Natl Acad Sci USA **100**: 2975–2980

Lévy J, Bres C, Geurts R, Chalhoub B, Kulikova O, Duc G, Journet EP, Ané JM, Lauber E, Bisseling T, et al (2004) A putative Ca^{2+} and calmodulin-dependent protein kinase required for bacterial and fungal symbioses. Science **303**: 1361–1364

Mazars C, Bourque S, Mithöfer A, Pugin A, Ranjeva R (2009) Calcium homeostasis in plant cell nuclei. New Phytol **181**: 261–274

Messinese E, Mun JH, Yeun LH, Jayaraman D, Rouge P, Barre A, Lougnon G, Schornack S, Bono JJ, Cook DR, et al (2007) A novel nuclear protein interacts with the symbiotic DMI3 calcium- and calmodulin-dependent protein kinase of *Medicago truncatula*. Mol Plant Microbe Interact **20**: 912–921

Middleton PH, Jakab J, Penmetsa RV, Starker CG, Doll J, Kaló P, Prabhu R, Marsh JF, Mitra RM, Kereszt A, et al (2007) An ERF transcription factor in *Medicago truncatula* that is essential for Nod factor signal transduction. Plant Cell **19**: 1221–1234

Miwa H, Sun J, Oldroyd GED, Downie JA (2006) Analysis of calcium spiking using a cameleon calcium sensor reveals that nodulation gene expression is regulated by calcium spike number and the developmental status of the cell. Plant J **48**: 883–894

Miyawaki A, Griesbeck O, Heim R, Tsien RY (1999) Dynamic and quantitative Ca^{2+} measurements using improved cameleons. Proc Natl Acad Sci USA **96**: 2135–2140

Miyawaki A, Llopis J, Heim R, McCaffery JM, Adams JA, Ikura M, Tsien RY (1997) Fluorescent indicators for Ca^{2+} based on green fluorescent proteins and calmodulin. Nature **388**: 882–887

Oldroyd GE, Downie JA (2004) Calcium, kinases and nodulation signalling in legumes. Nat Rev Mol Cell Biol **5**: 566–576

Oldroyd GE, Downie JA (2006) Nuclear calcium changes at the core of symbiosis signalling. Curr Opin Plant Biol **9**: 351–357

Oldroyd GE, Downie JA (2008) Coordinating nodule morphogenesis with rhizobial infection in legumes. Annu Rev Plant Biol **59**: 519–546

Peiter E, Sun J, Heckmann AB, Venkateshwaran M, Riely BK, Otegui MS, Edwards A, Freshour G, Hahn MG, Cook DR, et al (2007) The *Medicago truncatula* DMI1 protein modulates cytosolic calcium signaling. Plant Physiol **145**: 192–203

Riely BK, Lougnon G, Ané JM, Cook DR (2007) The symbiotic ion channel homolog DMI1 is localized in the nuclear membrane of *Medicago truncatula* roots. Plant J **49**: 208–216

Saito K, Yoshikawa M, Yano K, Miwa H, Uchida H, Asamizu E, Sato S, Tabata S, Imaizumi-Anraku H, Umehara Y, et al (2007) NUCLEOPORIN85 is required for calcium spiking, fungal and bacterial symbioses, and seed production in *Lotus japonicus*. Plant Cell **19**: 610–624

Shaw SL, Long SR (2003) Nod factor elicits two separable calcium responses in *Medicago truncatula* root hair cells. Plant Physiol **131**: 976–984

Smit P, Raedts J, Portyanko V, Debellé F, Gough C, Bisseling T, Geurts R (2005) NSP1 of the GRAS protein family is essential for rhizobial Nod factor-induced transcription. Science **308**: 1789–1791

Wais RJ, David H, Keating DH, Long SR (2002) Structure-function analysis of Nod factor-induced root hair calcium spiking in Rhizobium-legume symbiosis. Plant Physiol **129**: 211–224

Wais RJ, Galera C, Oldroyd G, Catoira R, Penmetsa RV, Cook D, Gough C, Denarie J, Long SR (2000) Genetic analysis of calcium spiking responses in nodulation mutants of *Medicago truncatula*. Proc Natl Acad Sci USA **97**: 13407–13412

Watahiki M, Trewavas AJ, Parton RM (2004) Fluctuations in the pollen tube tip-focused calcium gradient are not reflected in nuclear calcium level: a comparative analysis using recombinant yellow cameleon calcium reporter. Sex Plant Reprod **17**: 125–130

Yano K, Yoshida S, Müller J, Singh S, Banba M, Vickers K, Markmann K, White C, Schuller B, Sato S, et al (2008) CYCLOPS, a mediator of symbiotic intracellular accommodation. Proc Natl Acad Sci USA **105**: 20540–20545